

Heterotrimeric G Proteins Serve as a Converging Point in Plant Defense Signaling Activated by Multiple Receptor-Like Kinases^{1[C][W][OA]}

Jinman Liu^{2,3}, Pingtao Ding², Tongjun Sun, Yukino Nitta, Oliver Dong, Xingchuan Huang, Wei Yang, Xin Li, José Ramón Botella, and Yuelin Zhang*

National Institute of Biological Sciences, Zhongguancun Life Science Park, Beijing 102206, China (J.L., P.D., X.H., W.Y., Y.Z.); College of Life Sciences, Beijing Normal University, Beijing 100875, China (P.D.); Department of Botany, University of British Columbia, Vancouver, Canada V6T 1Z4 (P.D., T.S., Y.N., O.D., X.L., Y.Z.); and Plant Genetic Engineering Laboratory, School of Agriculture and Food Sciences, University of Queensland, Brisbane, Queensland 4072, Australia (J.R.B.)

In fungi and metazoans, extracellular signals are often perceived by G-protein-coupled receptors (GPCRs) and transduced through heterotrimeric G-protein complexes to downstream targets. Plant heterotrimeric G proteins are also involved in diverse biological processes, but little is known about their upstream receptors. Moreover, the presence of bona fide GPCRs in plants is yet to be established. In *Arabidopsis* (*Arabidopsis thaliana*), heterotrimeric G protein consists of one G α subunit (G PROTEIN α -SUBUNIT1), one G β subunit (ARABIDOPSIS G PROTEIN β -SUBUNIT1 [AGB1]), and three G γ s subunits (ARABIDOPSIS G PROTEIN γ -SUBUNIT1 [AGG1], AGG2, and AGG3). We identified AGB1 from a suppressor screen of *BAK1-interacting receptor-like kinase1-1* (*bir1-1*), a mutant that activates cell death and defense responses mediated by the receptor-like kinase (RLK) SUPPRESSOR OF BIR1-1. Mutations in AGB1 suppress the cell death and defense responses in *bir1-1* and transgenic plants overexpressing SUPPRESSOR OF BIR1-1. In addition, *agb1* mutant plants were severely compromised in immunity mediated by three other RLKs, FLAGELLIN-SENSITIVE2 (FLS2), Elongation Factor-TU RECEPTOR (EFR), and CHITIN ELICITOR RECEPTOR KINASE1 (CERK1), respectively. By contrast, G PROTEIN α -SUBUNIT1 is not required for either cell death in *bir1-1* or pathogen-associated molecular pattern-triggered immunity mediated by FLS2, EFR, and CERK1. Further analysis of *agg1* and *agg2* mutant plants indicates that AGG1 and AGG2 are also required for pathogen-associated molecular pattern-triggered immune responses mediated by FLS2, EFR, and CERK1, as well as cell death and defense responses in *bir1-1*. We hypothesize that the *Arabidopsis* heterotrimeric G proteins function as a converging point of plant defense signaling by mediating responses initiated by multiple RLKs, which may fulfill equivalent roles to GPCRs in fungi and animals.

Receptor-like kinases (RLKs) represent one of the largest protein families in plants and play diverse roles in plant development and stress signaling (Morillo and Tax, 2006). In *Arabidopsis* (*Arabidopsis thaliana*), there are over 600 RLKs (Shiu and Blecker, 2001). Most RLKs contain an extracellular domain, a

single transmembrane motif, and a cytoplasmic kinase domain. It is believed that the extracellular domains are involved in ligand recognition that subsequently leads to activation of the cytoplasmic kinase domain. Pathogen-associated molecular pattern (PAMP) receptors FLAGELLIN-SENSITIVE2 (FLS2), Elongation Factor (EF)-TU RECEPTOR (EFR), and CHITIN ELICITOR RECEPTOR KINASE1 (CERK1) all belong to the RLK family. FLS2 and EFR function as receptors for bacterial flagellin and EF-Tu, respectively (Gómez-Gómez and Boller, 2000; Zipfel et al., 2006), while CERK1 is involved in the perception of chitin, a common component of the fungal cell wall (Miya et al., 2007; Wan et al., 2008). CERK1 was also shown to play an important role in defense against bacterial pathogens (Gimenez-Ibanez et al., 2009). Another RLK, Brassinosteroid Insensitive1-associated receptor kinase1 (BAK1), functions as a coreceptor for FLS2 and EFR (Chinchilla et al., 2007; Heese et al., 2007). In addition, a rice (*Oryza sativa*) RLK, Xa21, functions as the receptor for a peptide derived from AvrXa21 (Song et al., 1995; Lee et al., 2009).

Activation of different PAMP receptors often leads to rapid downstream responses, such as oxidative burst,

¹ This work was supported by funding from the Natural Sciences and Engineering Research Council of Canada and the Chinese Ministry of Science and Technology (grant no. 2011CB100700).

² These authors contributed equally to the article.

³ Present address: University of Oklahoma Health Sciences Center, Biomedical Research Center 366, 975 NE 10th St., Oklahoma City, OK 73104.

* Corresponding author; e-mail yuelin.zhang@ubc.ca.

The author responsible for distribution of materials integral to the findings presented in this article in accordance with the policy described in the Instructions for Authors (www.plantphysiol.org) is: Yuelin Zhang (yuelin.zhang@ubc.ca).

[C] Some figures in this article are displayed in color online but in black and white in the print edition.

[W] The online version of this article contains Web-only data.

[OA] Open Access articles can be viewed online without a subscription.

www.plantphysiol.org/cgi/doi/10.1104/pp.112.212431

calcium influx, mitogen-activated protein kinase (MAPK) activations, and the up-regulation of defense gene expression (Boller and Felix, 2009). However, our knowledge of how defense responses are regulated downstream of the RLKs remains limited. Genetic analysis of mutants defective in EFR-mediated PAMP responses showed that endoplasmic reticulum (ER) quality control plays an important role in the accumulation of EFR (Li et al., 2009; Lu et al., 2009; Nekrasov et al., 2009; Saijo et al., 2009). ER-resident chaperones are also required for the accumulation of the tobacco (*Nicotiana tabacum*) INDUCED RECEPTOR-LIKE KINASE (Caplan et al., 2009). *BOTRYTIS-INDUCED KINASE1* (*BIK1*) encodes a cytoplasmic RLK that directly interacts with FLS2 and likely EFR and CERK1 (Lu et al., 2010; Zhang et al., 2010). Knocking out *BIK1* leads to modest reductions of PAMP-induced callose deposition, H₂O₂ accumulation, and pathogen resistance. Recently, a group of redundant calcium-dependent protein kinases (CDPKs) were identified as critical regulators of MAPK-independent defense pathways downstream of FLS2 (Boudsocq et al., 2010).

In yeast (*Saccharomyces cerevisiae*) and metazoans, heterotrimeric G proteins, composed of α -, β -, and γ -subunits, serve as essential signaling intermediates between cell surface G-protein-coupled receptors (GPCRs) and their downstream targets (Temple and Jones, 2007). Binding of ligands to GPCRs leads to the exchange of GDP for GTP in the α -subunit, resulting in the activation of the G protein. In Arabidopsis, there is one $G\alpha$ subunit (G PROTEIN α -SUBUNIT1 [GPA1]), one $G\beta$ subunit (ARABIDOPSIS G PROTEIN β -SUBUNIT1 [AGB1]), and three $G\gamma$ subunits (ARABIDOPSIS G PROTEIN γ -SUBUNIT1 [AGG1], AGG2, and AGG3; Temple and Jones, 2007; Chakravorty et al., 2011). Whereas AGG1 and AGG2 are closely related, AGG3 only shares very limited homology to AGG1 and AGG2. GPCR-like proteins have been identified in plants, and their interactions with $G\alpha$ have been experimentally proven, although their status as bona fide GPCRs remains controversial (Liu et al., 2007; Gookin et al., 2008; Pandey et al., 2009).

Heterotrimeric G proteins have been shown to be involved in a wide range of biological processes, including plant immunity (Perfus-Barbeoch et al., 2004). Analysis of rice *dwarf1* mutants with defects in the $G\alpha$ subunit indicates that the rice $G\alpha$ subunit plays an important role in resistance against rice blast (Suharsono et al., 2002). In Arabidopsis, loss of function of the $G\beta$ or $G\gamma$ subunits leads to compromised resistance against the necrotrophic pathogen *Plectosphaerella cucumerina* (Llorente et al., 2005; Delgado-Cerezo et al., 2012). By contrast, loss of function of the $G\alpha$ subunit GPA1 results in enhanced resistance against the pathogen (Llorente et al., 2005). Resistance against other necrotrophic pathogens, such as *Fusarium oxysporum*, *Alternaria brassicicola*, and *Botrytis cinerea*, was also found to be compromised in AGB1- and AGG1/AGG2-deficient mutants (Trusov et al., 2006, 2007, 2009). In addition, loss of function of the $G\beta$ subunit

leads to reduced elf18-induced resistance against *Agrobacterium tumefaciens* as well as reduced reactive oxygen species (ROS) production triggered by flagellin22 (flg22) and elf18 (an 18-amino acid peptide that represents the N terminus of bacterial EF-Tu; Ishikawa, 2009). Multiple surface residues of AGB1 were recently shown to play important roles in resistance against necrotrophic pathogens and flg22-induced ROS production (Jiang et al., 2012).

Arabidopsis GPA1 was also found to play an important role in stomatal defense. In *gpa1* mutants, flg22-induced inhibition of stomatal opening and inward K⁺ channels in guard cells are blocked (Zhang et al., 2008b). Growth of the coronatine-deficient *Pseudomonas syringae* pv *tomato* DC3118 is dramatically increased in *gpa1* mutant plants (Zeng and He, 2010). In *Nicotiana benthamiana*, silencing of the $G\alpha$ and $G\beta$ subunits also leads to reduced elicitor-induced stomatal closure as well as hypersensitive responses induced by harpin (Zhang et al., 2012a).

Arabidopsis *BAK1-INTERACTING RECEPTOR-LIKE KINASE1* (*BIR1*) encodes a BAK1-associated RLK (Gao et al., 2009). Knocking out *BIR1* results in constitutive activation of cell death and defense responses in a manner that is partially dependent on PHYTOALEXIN DEFICIENT4 (*PAD4*), a positive regulator of resistance mediated by the Toll-Interleukin-1 Receptor-like-Nucleotide-Binding-Leu-Rich Repeat domain class of resistance proteins. To identify signaling components downstream of *BIR1*, a suppressor screen was performed in the *bir1-1 pad4-1* double-mutant background. A number of suppressor of *bir1-1* (*sobir*) mutants suppressing the seedling lethality phenotype of *bir1-1* were identified. *SOBIR1* encodes another RLK whose overexpression is sufficient to activate cell death and defense responses (Gao et al., 2009). Combining the *sobir1-1* and *pad4-1* mutations results in complete suppression of cell death and enhanced pathogen resistance in *bir1-1*, suggesting that *SOBIR1* and *PAD4* function in parallel to regulate cell death and defense responses. Here, we report the discovery and characterization of *SOBIR2*, which encodes the Arabidopsis heterotrimeric G-protein β -subunit AGB1 that functions downstream of *SOBIR1* to regulate cell death and defense responses.

RESULTS

Identification and Characterization of *sobir2-1 bir1-1 pad4-1*

The *sobir2-1* mutant was identified from a suppressor screen in the *bir1-1 pad4-1* background as previously described (Gao et al., 2009). The *sobir2-1 bir1-1 pad4-1* triple mutant is significantly larger than *bir1-1 pad4-1* (Fig. 1A) and can easily grow to maturity and set seeds at 23°C. The expression levels of defense marker genes *PATHOGENESIS-RELATED1* (*PR1*; Fig. 1B) and *PR2* (Fig. 1C) in *sobir2-1 bir1-1 pad4-1* are considerably lower than those in *bir1-1 pad4-1*. In addition, enhanced resistance to *Hyaloperonospora arabidopsidis* Noco2 in *bir1-1*

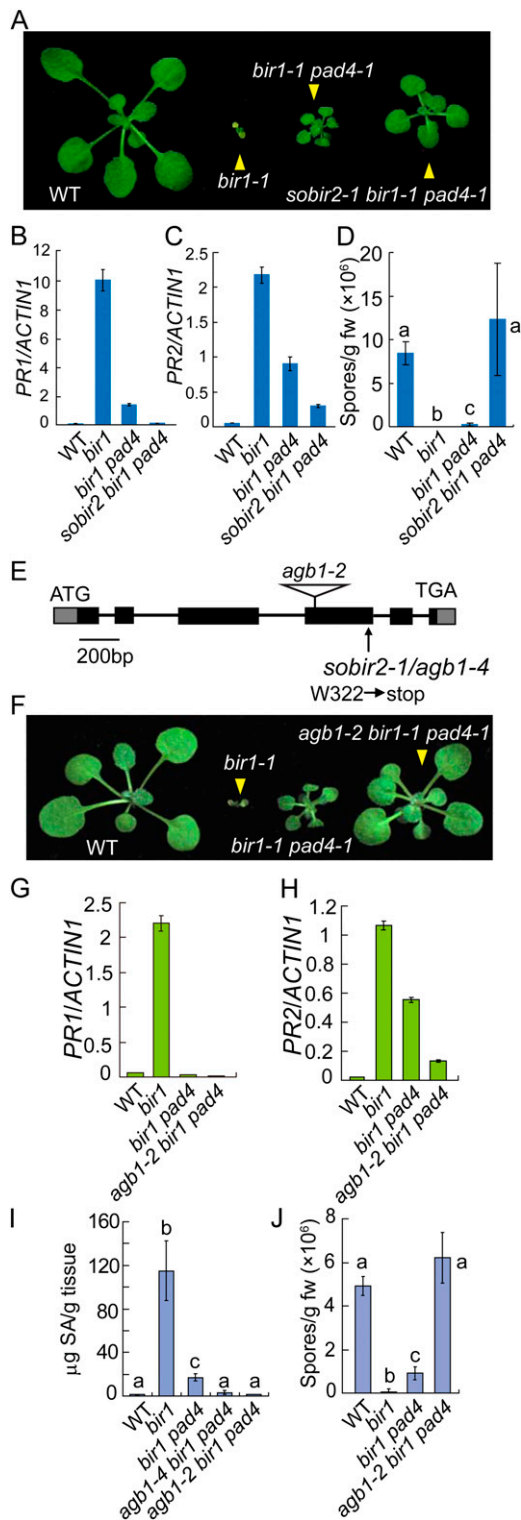


Figure 1. Characterization and cloning of *sobir2-1*. A, Morphology of wild-type, *bir1-1*, *bir1-1 pad4-1*, and *sobir2-1 bir1-1 pad4-1* plants. Plants were grown on soil at 23°C and photographed about 3 weeks after planting. B and C, *PR1* (B) and *PR2* (C) expression in wild-type, *bir1-1*, *bir1-1 pad4-1*, and *sobir2-1 bir1-1 pad4-1* seedlings. Values were normalized to the expression of *ACTIN1*. Error bars represent sds from means of three measurements. D, Growth of *H. arabidopsidis*

pad4-1 is completely abolished in the *sobir2-1 bir1-1 pad4-1* triple mutant (Fig. 1D). Taken together, our data show that *sobir2-1* suppresses the constitutive defense responses observed in *bir1-1 pad4-1*.

SOBIR2 Encodes the Heterotrimeric G-Protein β -Subunit

To map the *sobir2-1* mutation, *sobir2-1 bir1-1 pad4-1* (in the Columbia ecotype background) was crossed with the Landsberg *erecta* ecotype to generate a segregating mapping population. Crude mapping using the F2 progeny showed that the *sobir2-1* mutation is located between marker T16L1 and F8D20 on chromosome 4. Further fine mapping narrowed the *sobir2-1* mutation to a 40-kb region between markers F10M10 and T4L20 (Supplemental Fig. S1). Sequence analysis of genes in this region in the *sobir2-1* mutant identified a single G-to-A mutation in *At4g34460*, which encodes the heterotrimeric G-protein β -subunit. The mutation created an early stop codon in the gene (Fig. 1E); thus, *sobir2-1* was renamed *agb1-4*. Semiquantitative reverse transcription (RT)-PCR analysis showed that *AGB1* is expressed at a slightly lower level in *agb1-4* compared with the wild type (Supplemental Fig. S2), suggesting that a truncated *AGB1* protein may still be expressed in the mutant. Whether the truncated protein retains part of the function of *AGB1* is unclear.

To confirm that the mutation in *At4g34460* causes suppression of the *bir1-1* phenotypes, we crossed *agb1-2* into *bir1-1 pad4-1*. *agb1-2* contains a transfer DNA insertion that disrupts the expression of *AGB1* (Supplemental Fig. S2). The *agb1-2 bir1-1 pad4-1* triple mutant restored the size and appearance of *bir1-1 pad4-1* to almost wild-type levels (Fig. 1F), suggesting that *SOBIR2* encodes *AGB1*. Further analysis showed that expression of both *PR1* and *PR2* was dramatically reduced in the triple mutant (Fig. 1, G and H). In both *agb1-4 bir1-1 pad4-1* and *agb1-2 bir1-1 pad4-1*, the levels of salicylic acid (SA) were much lower than those in *bir1-1* and *bir1-1 pad4-1* (Fig. 1I). In addition, enhanced resistance to *H. arabidopsidis* Noco2 in *bir1-1 pad4-1* was completely lost in *agb1-2 bir1-1 pad4-1* (Fig. 1J).

Noco2 on the wild type, *bir1-1*, *bir1-1 pad4-1*, and *sobir2-1 bir1-1 pad4-1*. E, Predicted gene structure of *SOBIR2/AGB1*. Boxes are exons, and lines indicate introns. The ATG start and TGA stop codons are indicated. F, Morphology of the wild type, *bir1-1*, *bir1-1 pad4-1*, and *agb1-2 bir1-1 pad4-1*. G and H, *PR1* (G) and *PR2* (H) expression in the wild type, *bir1-1*, *bir1-1 pad4-1*, and *agb1-2 bir1-1 pad4-1*. Values were normalized to the expression of *ACTIN1*. Error bars represent sds from means of three measurements. I, Total SA levels in the wild type, *bir1-1*, *bir1-1 pad4-1*, *agb1-4 bir1-1 pad4-1*, and *agb1-2 bir1-1 pad4-1*. Statistical differences among different genotypes are labeled with different letters ($P < 0.01$). J, Growth of *H. arabidopsidis* Noco2 on the wild type, *bir1-1*, *bir1-1 pad4-1*, and *agb1-2 bir1-1 pad4-1*. Statistical differences among different genotypes are labeled with different letters ($P < 0.001$). WT, Wild type. [See online article for color version of this figure.]

Mutations in *AGB1* Suppress Cell Death and Defense Responses in *bir1-1*

To determine whether mutations in *AGB1* can suppress the cell death and defense responses in *bir1-1*, we obtained the *agb1-4 bir1-1* double mutant by crossing *agb1-4 bir1-1 pad4-1* with wild-type Columbia and *agb1-2 bir1-1* by crossing *agb1-2* and *bir1-1*. Unlike *bir1-1* mutant plants, *agb1-4 bir1-1* and *agb1-2 bir1-1* can grow to maturity and set seeds at 23°C. *agb1-4 bir1-1* and *agb1-2 bir1-1* are much larger than *bir1-1*, though smaller than the wild type (Fig. 2A). To determine whether cell death was blocked in the double mutants, trypan blue staining was performed on seedlings. As shown in Figure 2B, cell death in *bir1-1* was inhibited by the *agb1-4* and *agb1-2* mutations. Accumulation of H₂O₂ in *bir1-1* was also partially blocked in *agb1-4 bir1-1* and *agb1-2 bir1-1* (Supplemental Fig. S3). In addition, constitutive expression of *PR1* in *bir1-1* was dramatically reduced in the double mutants (Fig. 2C), whereas the expression of *PR2* was only modestly reduced (Fig. 2D), suggesting that cell death is a major contributor to the activation of *PR1* expression and the expression of *PR2* is largely independent of cell death in *bir1-1*. Both *agb1-4 bir1-1* and *agb1-2 bir1-1* accumulated less SA than *bir1-1*, but SA levels in the double mutants were still much higher than that in the wild type (Fig. 2E). Consistent with the reduced SA levels, *agb1-4 bir1-1* and *agb1-2 bir1-1* supported much higher growth of *H. arabidopsidis* Noco2 than *bir1-1*, but supported less growth of the pathogen than the wild type (Fig. 2F).

AGB1 Is Required for Cell Death in Transgenic Plants Overexpressing *SOBIR1*

It was previously shown that *bir1-1* activates *SOBIR1*-dependent cell death (Gao et al., 2009). To test whether *AGB1* functions downstream of *SOBIR1*, we introduced the *agb1-2* mutation into *SOBIR1* overexpression (*OX-2*), a transgenic line overexpressing *SOBIR1* that exhibits spontaneous cell death (Gao et al., 2009). Semiquantitative RT-PCR analysis indicates that *SOBIR1* is expressed at similar levels in the wild type and *agb1-2* carrying the 35S-*SOBIR1* transgene (Supplemental Fig. S4). As shown in Figure 3A, *agb1-2* partially suppresses the dwarf phenotype of the *SOBIR1* overexpression line. Trypan blue staining showed that cell death in the transgenic line was suppressed by *agb1-2* (Fig. 3B), suggesting that *AGB1* functions downstream of the RLK *SOBIR1* to regulate cell death.

AGB1 Is Required for PAMP-Mediated Immunity

To determine whether *AGB1* is also required for resistance responses mediated by three other RLKs, *FLS2*, *EFR*, and *CERK1*, we first analyzed bacterial growth in wild-type and *agb1-2* plants pretreated with flg22, a peptide derived from bacterial flagellin that is recognized by *FLS2* (Gómez-Gómez and Boller, 2000). As

shown in Figure 3C, flg22-induced resistance to *P. syringae* pv *tomato* DC3000 was blocked in *agb1-2* compared with wild-type plants. Analysis of bacterial growth in the wild type and *agb1-2* treated with elf18, a peptide derived from bacterial EF-Tu, showed that elf18-induced resistance to *P. syringae* pv *tomato* DC3000 was also reduced in *agb1-2* (Fig. 3D). Furthermore, chitin-induced resistance to *P. syringae* pv *tomato* DC3000 was lost in *agb1-2* as well (Fig. 3E). By contrast, flg22-, elf18-, and chitin-induced resistance to *P. syringae* pv *tomato* DC3000 was not impaired in the $G\alpha$ mutant *gpa1-3* (Fig. 3, C–E). The reduction in PAMP-induced resistance observed in *agb1-2* can be complemented by expressing the wild-type *AGB1* with a C-terminal FLAG tag. These results suggest that *AGB1* is required for PAMP-triggered immunity mediated by the RLKs *FLS2*, *EFR*, and *CERK1*.

Next, we tested whether induction of ROS production by flg22 and elf18 was affected in *agb1-2*. As shown in Figure 3, F and G, flg22- and elf18-induced ROS production was clearly reduced in the mutant, consistent with the previous report that ROS production induced by flg22 and elf18 was reduced in *agb1-2* (Ishikawa, 2009). We further tested whether induction of ROS production by chitin is affected in *agb1-2*. As shown in Figure 3H, chitin-induced ROS production was also reduced in *agb1-2*. These data suggest that *AGB1* is required for PAMP-triggered induction of ROS. The *gpa1-3* mutant lacking the $G\alpha$ subunit has little or no effect on ROS induction by flg22, elf18, or chitin.

To test whether *AGB1* functions as a general regulator of the stability of PAMP receptors, we analyzed the accumulation of *FLS2* in *agb1-2* and *agb1-4* by western-blot analysis. As shown in Supplemental Figure S5, the levels of *FLS2* protein in *agb1-2* and *agb1-4* were comparable in the wild type and the *agb1* mutants, suggesting that *AGB1* is not required for the accumulation of *FLS2*.

To test whether activation of the MAPKs *MPK3* and *MPK6* by flg22 is affected by *agb1-2*, we analyzed phosphorylated *MPK3* and *MPK6* in plants treated with flg22 by western blot using an anti-Erk1/2 (for Extracellular signal-regulated kinase) antibody specific for phosphorylated MAPKs. As shown in Figure 3I and Supplemental Figure S6, flg22-induced activation of *MPK3* and *MPK6* was not affected in the mutant, which is consistent with the previous report that activation of *MPK3* and *MPK6* by flg22 was not affected by *agb1-2* (Ishikawa, 2009). We further tested whether *agb1-2* affects flg22-induced expression of *FLG22-INDUCED RECEPTOR-LIKE KINASE1* (*FRK1*) and *WRKY DNA-BINDING PROTEIN29* (*WRKY29*), two marker genes for activation of the *MPK3/MPK6*-signaling pathway. As shown in Supplemental Figure S7, induction of these two genes was not affected in *agb1-2* either, suggesting that *AGB1* functions in a defense pathway independent of *MPK3* and *MPK6*.

Next, we tested whether activation of *MPK4* by flg22 is affected by mutations in *AGB1*. *MPK4* was immunoprecipitated from the wild type and *agb1* mutants using anti-*MPK4* antibodies and assayed for its kinase activity using myelin basic protein (MBP) as a substrate. As shown in Figure 3J, activation of *MPK4* was

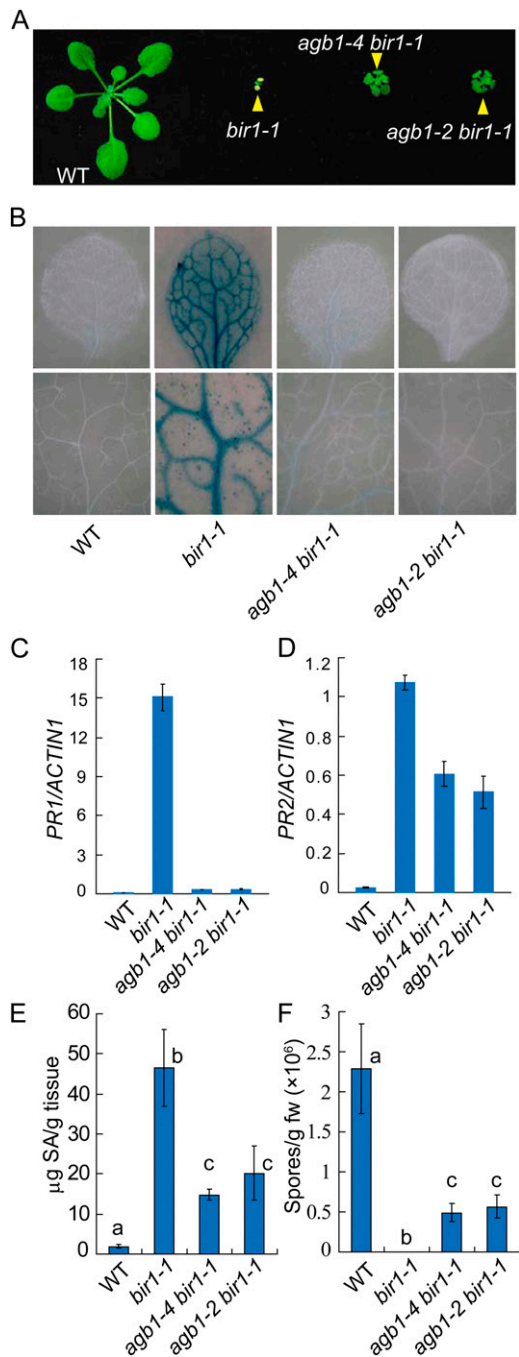


Figure 2. Suppression of cell death and defense responses in *bir1-1* by *agb1-4* and *agb1-2*. A, Morphology of wild-type, *bir1-1*, *agb1-4 bir1-1*, and *agb1-2 bir1-1* plants. Plants were grown on soil at 23°C and photographed about 3 weeks after planting. B, Trypan blue staining of the wild-type, *bir1-1*, *agb1-4 bir1-1*, and *agb1-2 bir1-1* mutant seedlings. Plants were grown at 23°C for 2 weeks on one-half-strength MS plates. C and D, *PR1* (C) and *PR2* (D) expression in the wild type, *bir1-1*, *agb1-4 bir1-1*, and *agb1-2 bir1-1*. Values were normalized to the expression of *ACTIN1*. Error bars represent sds from means of three measurements. E, Total SA levels in the wild type, *bir1-1*, *agb1-4 bir1-1*, and *agb1-2 bir1-1*. Statistical differences among different genotypes are labeled with different letters ($P < 0.01$). F, Growth of *H. arabidopsis* Noco2 on the wild type, *bir1-1*, *agb1-4 bir1-1*, and *agb1-2*

reduced in both *agb1-2* and *agb1-4*, suggesting that AGB1 is required for full activation of MPK4.

Both MAPK-dependent and independent signaling pathways are activated during PAMP signaling. Induction of *GLUTATHIONE S-TRANSFERASE1* (*GST1*) expression by flg22 was previously shown to be independent of MAPK signaling (Asai et al., 2002). To determine whether AGB1 is required for induction of *GST1* by flg22, we compared the expression levels of *GST1* in flg22-treated wild-type and *agb1-2* plants. As shown in Supplemental Figure S8, induction of *GST1* by flg22 was not affected in the *agb1-2* mutant.

The *agg1 agg2* Double Mutant Suppresses Cell Death in *bir1-1*

Next, we tested whether the G-protein subunits $G\alpha$ and $G\gamma$ are also required for cell death and defense responses in *bir1-1*. The *gpa1-3 bir1-1*, *gpa1-4 bir1-1*, *agg1-1c bir1-1*, and *agg2-1 bir1-1* double mutants and the *agg1-1c agg2-1 bir1-1* triple mutant were obtained by crossing *bir1-1* with *gpa1-3*, *gpa1-4*, and *agg1-1c agg2-1*, respectively. As shown in Supplemental Figure S9, *gpa1-3 bir1-1* and *gpa1-4 bir1-1* exhibited morphology similar to *bir1-1* and were seedling lethal, suggesting that GPA1 is dispensable for the seedling lethality phenotype of *bir1-1*. Both *agg1-1c bir1-1* and *agg2-1 bir1-1* show slightly increased size compared with *bir1-1* (Fig. 4A). By contrast, the *agg1-1c agg2-1 bir1-1* triple mutant is much bigger than *bir1-1* and is able to complete its life cycle at 23°C, suggesting that AGG1 and AGG2 function redundantly to regulate cell death in *bir1-1*. Suppression of cell death in *bir1-1* by *agg1-1c agg2-1* was further confirmed by trypan blue staining (Fig. 4B). Real-time RT-PCR analysis showed that the constitutive expression of *PR1*, but not *PR2*, was considerably reduced in *agg1-1c bir1-1* and *agg1-1c agg2-1 bir1-1* compared with *bir1-1* (Fig. 4, C and D). The *agg1-1c agg2-1 bir1-1* triple mutant also accumulated less SA (Fig. 4E) and supported much higher growth of *H. arabidopsis* Noco2 (Fig. 4F) than *bir1-1*. Taken together, AGG1 and AGG2 are required for the cell death and part of the constitutive defense response phenotypes in *bir1-1*.

AGG1 and AGG2 Are Involved in PAMP-Mediated Defense Responses

To determine whether AGG1 and/or AGG2 are also required for resistance responses mediated by the RLKs FLS2, EFR, and CERK1, we analyzed flg22-, elf18-, and chitin-induced resistance to *P. syringae* pv *tomato* DC3000 in the wild type, *agg1*, *agg2*, and the *agg1 agg2* double mutant. Treatment with flg22 (Fig. 5A), elf18 (Fig.

bir1-1. Statistical differences among different genotypes are labeled with different letters ($P < 0.001$). WT, Wild type. [See online article for color version of this figure.]

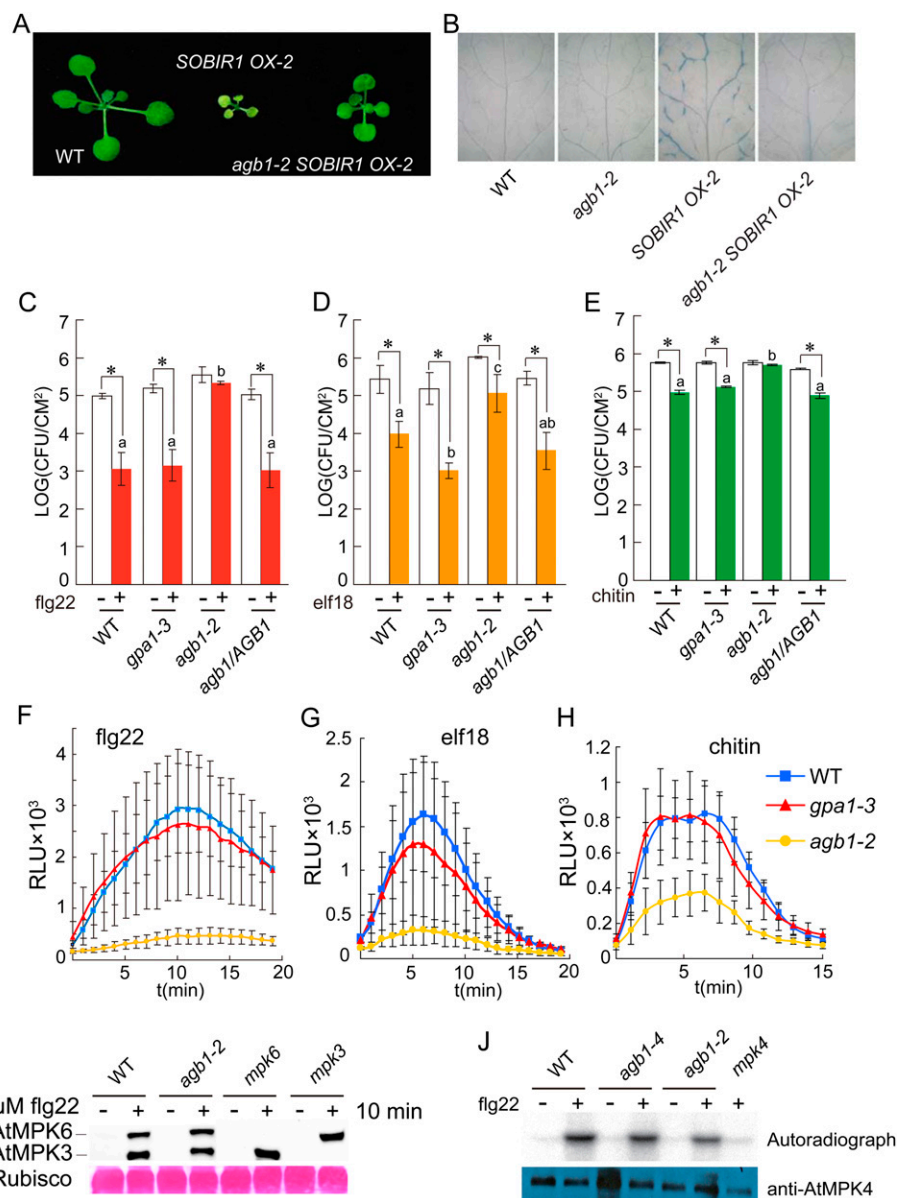


Figure 3. *agb1-2* suppresses cell death in transgenic plants overexpressing *SOBIR1* and compromised PAMP-triggered immunity. **A**, Morphology of the wild type, 35S-*SOBIR1* transgenic line number 2 (*SOBIR1 OX-2*; Gao et al., 2009), and *agb1-2* carrying the 35S-*SOBIR1* transgene from line number 2 (*agb1-2 SOBIR1 OX-2*). Plants were grown on soil at 23°C and photographed approximately 3 weeks after planting. **B**, Trypan blue staining of the indicated genotypes. Plants were grown at 23°C for 2 weeks on one-half-strength MS plates. **C** to **E**, flg22-induced (**C**), elf18-induced (**D**), or chitin-induced (**E**) resistance to *P. syringae* pv *tomato* DC3000 in the wild type, *gpa1-3* (SALK_066823), *agb1-2*, and a transgenic line expressing *AGB1* under its own promoter in *agb1-2* background (*agb1/AGB1*). Plants were pretreated with the indicated PAMPs (+) or water (–) 1 d before infiltration with *P. syringae* pv *tomato* DC3000 (OD₆₀₀ = 0.001). Bacterial titers on day 3 are shown. Error bars represent sds from means of six measurements. Asterisks above the bars indicate significant difference between samples treated with or without the indicated elicitors (**P* < 0.01). Statistical differences among the elicitor-treated samples are labeled with different letters (*P* < 0.01). **F** to **H**, Oxidative burst triggered by flg22 (**F**), elf18 (**G**), or chitin (**H**) in the indicated genotypes. Leaf slices of 4-week-old plants were treated with 1 μM flg22, 1 μM elf18, or 200 μg mL⁻¹ chitin, and ROS was subsequently measured. Error bars represent sds from means of eight samples. **I**, Activation of MPK3 and MPK6 in the wild type and *agb1-2* by flg22. Two-week-old seedlings grown on one-half-strength MS medium were treated with or without 1 μM flg22. Phosphorylated MPK3 and MPK6 were detected by western blot using an anti-Erk1/2 antibody specific for the phosphorylated MAPKs. *mpk3* and *mpk6* knockout mutants were included as controls. **J**, Activation of MPK4 in the wild type and *agb1* mutants by flg22. Two-week-old seedlings grown on one-half-strength MS medium were treated with or without 1 μM flg22. MPK4 was immunoprecipitated from total protein extracts using anti-MPK4 antibodies (Sigma) and assayed for its kinase activity (autoradiograph) using MBP as the substrate. WT, Wild type. [See online article for color version of this figure.]

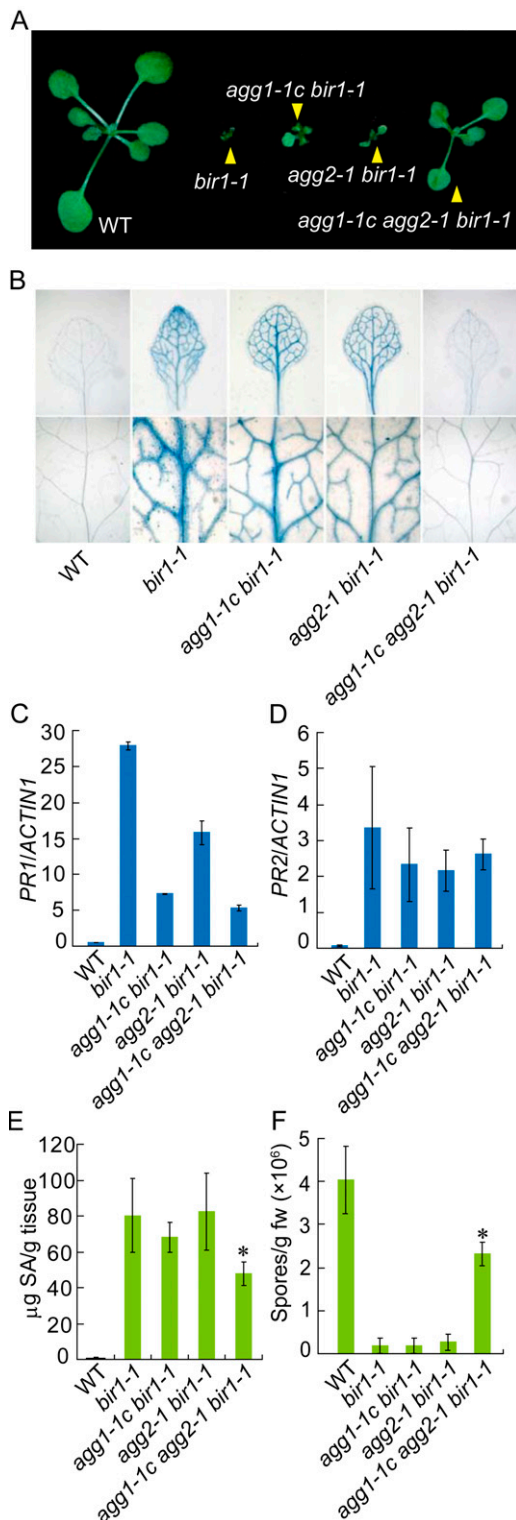


Figure 4. Suppression of cell death and defense responses in *bir1-1* by *agg1-1c agg2-1*. A, Morphology of wild-type, *bir1-1*, *agg1-1c bir1-1*, *agg2-1 bir1-1*, and *agg1-1c agg2-1 bir1-1* plants. Plants were grown on soil at 23°C and photographed when they were about 3 weeks old. B, Trypan blue staining of the indicated genotypes. Plants were grown at 23°C for 2 weeks on one-half-strength MS plates. C to D, *PR1* (C) and *PR2* (D) expression in the indicated genotypes. Values were

normalized to the expression of *ACTIN1*. Error bars represent sds from means of three measurements. E, SA levels in the indicated genotypes. Asterisks above the bars indicate significant difference from *bir1-1* (* $P < 0.01$). F, Growth of *H. arabidopsidis* Noco2 on the indicated genotypes. Asterisks above the bars indicate significant difference from *bir1-1* (* $P < 0.001$). WT, Wild type. [See online article for color version of this figure.]

5B), or chitin (Fig. 5C) resulted in reduction of bacterial growth in the wild type, *agg1-1c*, and *agg2-1*, but not in *agg1-1c agg2-1*, indicating that *flg22-*, *elf18-*, and chitin-induced resistance is blocked in the double mutant. Thus, *AGG1* and *AGG2* play redundant roles in the PAMP-mediated resistance induced by *flg22*, *elf18*, and chitin.

Next, we tested whether mutations in *AGG1* and *AGG2* affect PAMP-induced oxidative burst. In wild-type plants, treatment with *flg22*, *elf18*, or chitin leads to a rapid oxidative burst. As shown in Figure 5, D and F, the oxidative bursts triggered by *flg22* and chitin were not severely affected in either of the single $G\gamma$ mutants *agg1-1c* and *agg2-1*, but was dramatically reduced in the double *agg1-1c agg2-1* mutant. The *elf18*-induced oxidative burst was markedly reduced in *agg1-1c* and almost completely blocked in *agg1-1c agg2-1*, while *agg2-1* did not show any difference with the wild type (Fig. 5E). These data further support that *AGG1* and *AGG2* are critical signaling components in the response to *flg22*, *elf18*, and chitin.

We also analyzed *flg22*-induced activation of *MPK3* and *MPK6* in *agg1-1c*, *agg2-1*, and the *agg1-1c agg2-1* double mutant by western blot. As shown in Figure 5G and Supplemental Figure S10, activation of *MPK3* and *MPK6* was not affected in these mutants. We further tested whether activation of *MPK4* by *flg22* is affected in *agg1-1c*, *agg2-1*, and *agg1-1c agg2-1* mutant plants by assaying the kinase activity of *MPK4* from the wild type and the mutant plants. As shown in Figure 5H, activation of *MPK4* was reduced in the *agg1-1c agg2-1* double mutant, suggesting that *AGG1* and *AGG2* are also required for full activation of *MPK4*.

Next, we tested whether *flg22* induction of *GST1*, a marker gene activated independent of MAPK signaling, was affected in *agg1-1c*, *agg2-1*, and *agg1-1c agg2-1* mutant plants. As shown in Supplemental Figure S11, induction of *GST1* was comparable in the wild type and the mutant plants, suggesting that *AGG1* and *AGG2* are not required for the induction of *GST1* by *flg22*.

The $G\beta$ - and $G\gamma$ -Protein Subunits Are Required for Resistance against Nonpathogenic Bacteria

To further test whether *AGB1* and *GPA1* are required for PAMP-mediated resistance against nonpathogenic bacteria, we challenged *agb1-2* and *gpa1-4* with *P. syringae* pv *tomato* DC3000 *hrcC* (a nonpathogenic mutant defective in type III secretion). As shown in Figure 6A, growth of *P. syringae* pv *tomato* DC3000 *hrcC* is comparable in *gpa1-4* and wild-type plants, but is significantly higher in

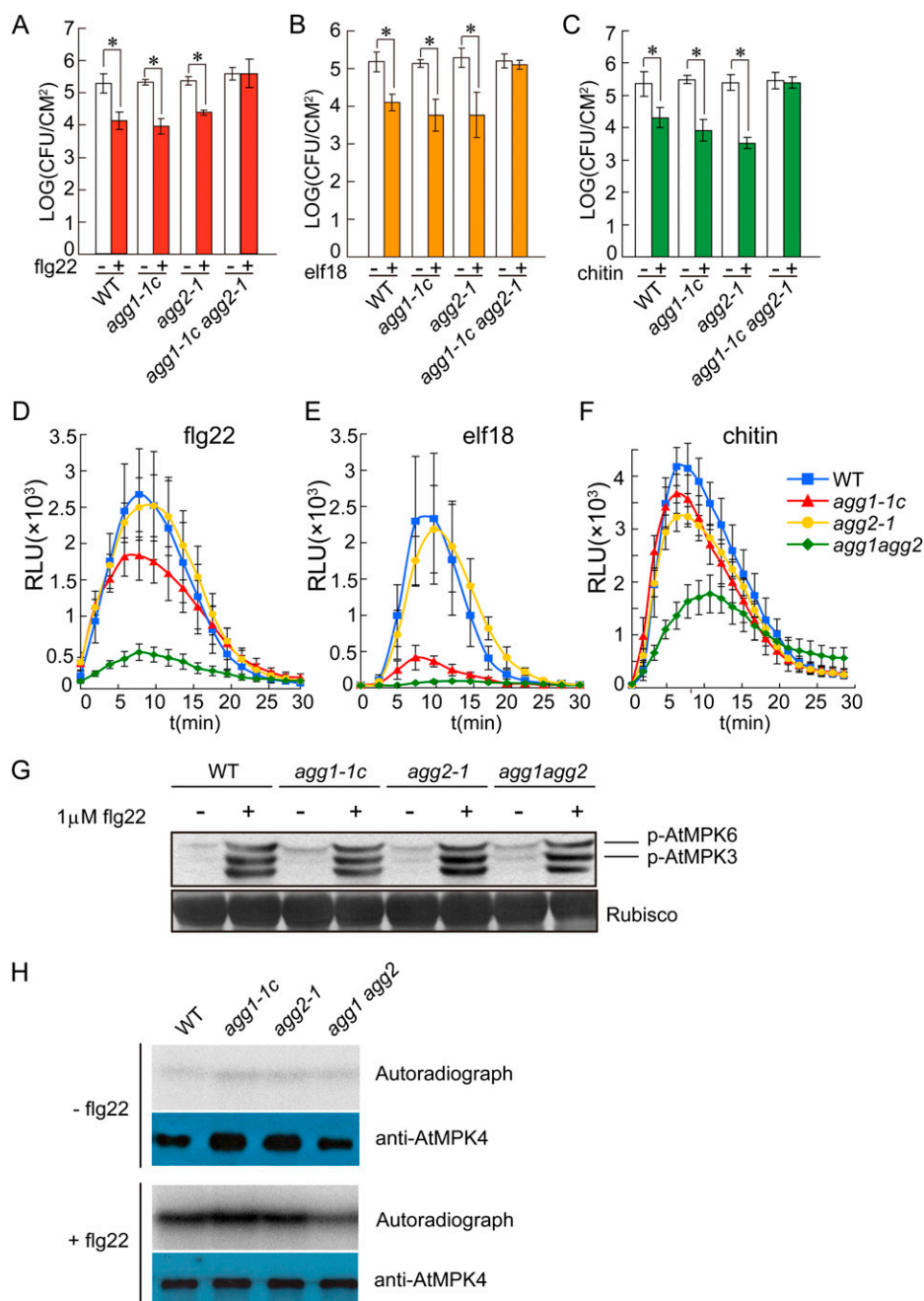


Figure 5. PAMP-triggered responses in the wild type, *agg1-1c*, *agg2-1*, and *agg1-1c agg2-1*. **A** to **C**, flg22-induced (A), elf18-induced (B), or chitin-induced (C) resistance to *P. syringae* pv *tomato* DC3000 in the wild type, *agg1-1c*, *agg2-1*, and *agg1-1c agg2-1*. Plants were pretreated with the indicated PAMP (+) or water (-) 1 d before infiltration with *P. syringae* pv *tomato* DC3000 ($OD_{600} = 0.001$). Bacterial titers on day 3 are shown. Error bars represent sds from means of six measurements. Asterisks above the bars indicate significant difference between samples treated with or without the indicated elicitors ($*P < 0.01$). **D** to **F**, Oxidative burst triggered by flg22 (A), elf18 (B), or chitin (C) in wild-type, *agg1-1c*, *agg2-1*, and *agg1-1c agg2-1* plants. Leaf slices of 4-week-old plants were treated with $1 \mu\text{M}$ flg22, $1 \mu\text{M}$ elf18, or $200 \mu\text{g mL}^{-1}$ chitin. ROS was measured using a luminol-dependent assay (Trujillo et al., 2008). Error bars represent sds from means of eight samples. **G**, Activation of MPK3 and MPK6 in the wild type, *agg1-1c*, *agg2-1*, and *agg1-1c agg2-1* by flg22. Two-week-old seedlings grown on one-half-strength MS medium were treated with or without $1 \mu\text{M}$ flg22. Phosphorylated MPK3 and MPK6 were detected by western blot using an anti-Erk1/2 antibody specific for the phosphorylated MAPKs. **H**, Activation of MPK4 in the wild type, *agg1-1c*, *agg2-1*, and *agg1-1c agg2-1* by flg22. Two-week-old seedlings were treated with or without $1 \mu\text{M}$ flg22. MPK4 was immunoprecipitated from total protein extracts using anti-MPK4 antibodies (Sigma) and assayed for its kinase activity (autoradiograph) using MBP as the substrate. WT, Wild type. [See online article for color version of this figure.]

agb1-2. We also challenged *agg1*, *agg2*, and *agg1 agg2* double-mutant plants with *P. syringae* pv *tomato* DC3000 *hrcC*. As shown in Figure 6B, growth of *P. syringae* pv *tomato* DC3000 *hrcC* is comparable in wild-type, *agg1-1c*, and *agg2-1* plants, but is about 3-fold higher in the *agg1-1c agg2-1* double mutant. These data suggest that $G\beta$ and $G\gamma$, but not $G\alpha$, are required for PAMP-mediated resistance against nonpathogenic bacteria.

FLS2 plays a very important role in stomatal defense against *P. syringae* pv *tomato* DC3000 (Melotto et al., 2006; Zeng and He, 2010). To test whether the $G\beta$ and $G\gamma$ subunits are required for stomatal defense, we sprayed

agb1-2, *agg1-1c*, *agg2-1*, *agg1-1c agg2-1*, and wild-type plants with *P. syringae* pv *tomato* DC3118, a *P. syringae* pv *tomato* DC3000 mutant deficient in the phytotoxin coronatine. Compared with wild-type plants, a small but significant increase of *P. syringae* pv *tomato* DC3118 growth was observed in *agb1-2* and *agg1-1c agg2-1* (Fig. 6C).

PAMP-Triggered Defense Responses Are Not Affected in *agg3* Single Mutants

To test whether the recently identified $G\gamma$ subunit AGG3 is required for PAMP-triggered defense responses,

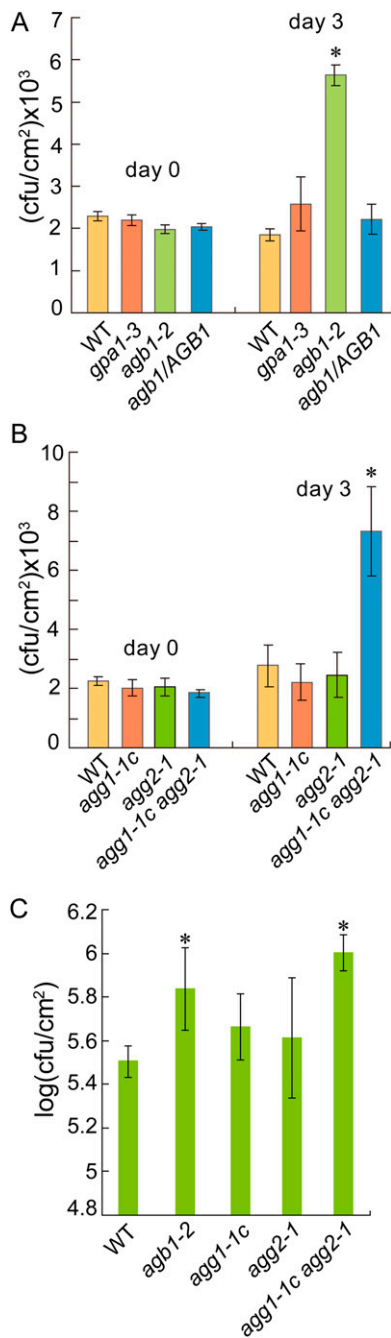


Figure 6. Growth of *P. syringae* pv *tomato* DC3000 *hrcC* and *P. syringae* pv *tomato* DC3118 in heterotrimeric G-protein mutants. A, Growth of *P. syringae* pv *tomato* DC3000 *hrcC* in the wild type, *gpa1-3*, *agb1-2*, and *agb1-2* expressing a wild-type *AGB1* transgene (*agb1/AGB1*). Asterisks above the bars indicate significant difference from the wild type ($*P < 0.01$). B, Growth of *P. syringae* pv *tomato* DC3000 *hrcC* in the wild type, *agg1-1c*, *agg2-1*, and *agg1-1c agg2-1*. Leaves of 6-week-old plants grown under short-day conditions (10-h day/14-h night cycles) were infiltrated with *P. syringae* pv *tomato* DC3000 *hrcC* ($OD_{600} = 0.002$). Bacterial titers at days 0 and 3 were measured by taking leaf discs within the inoculated area. Error bars represent sds from means of six samples. Asterisks above the bars indicate significant difference from the wild type ($*P < 0.01$). C, Growth of *P. syringae* pv *tomato* DC3118 in the wild type, *agb1-2*, *agg1-1c*, *agg2-1*, and *agg1-1c agg2-1*.

we analyzed induction of oxidative burst by *flg22*, *elf18*, and chitin in *agg3-1* and *agg3-2*. As shown in Supplemental Figure S12, A to C, oxidative bursts triggered by *flg22*, *elf18*, and chitin were not affected in the *agg3* mutants. Next, we tested *flg22*-induced resistance to *P. syringae* pv *tomato* DC3000 in *agg3-1* and *agg3-2*. As shown in Supplemental Figure S12D, resistance to *P. syringae* pv *tomato* DC3000 induced by *flg22* was not affected by the *agg3* mutations. In addition, growth of *P. syringae* pv *tomato* DC3000 *hrcC* was comparable in wild-type and *agg3* plants (Supplemental Fig. S12E). We also checked activation of MPK3 and MPK6 by *flg22* in the *agg3* mutants. As shown in Supplemental Figure S12F, activation of MPK3 and MPK6 by *flg22* was not affected in the *agg3* mutants either. These data suggest that PAMP-triggered defense responses are not affected in the *agg3* single-mutant plants.

DISCUSSION

Arabidopsis BIR1 negatively regulates two parallel defense pathways, one dependent on PAD4 and the other dependent on the RLK SOBIR1 (Gao et al., 2009). From a suppressor screen of *bir1-1*, we found that mutations in *AGB1* suppress cell death and defense responses in *bir1-1*. Combining mutations in *AGB1* and *PAD4* leads to more complete suppression of the mutant phenotypes and enhanced pathogen resistance in *bir1-1*, indicating that *AGB1* functions in parallel with *PAD4*. *AGB1* is also required for cell death in transgenic plants overexpressing *SOBIR1*, suggesting that the heterotrimeric G-protein β -subunit *AGB1* functions downstream of the RLK *SOBIR1* to regulate activation of cell death in *bir1-1*.

In *agb1* null mutant plants, induction of PAMP-triggered defense responses mediated by three other RLKs, *FLS2*, *EFR*, and *CERK1*, is severely compromised, suggesting that *AGB1* is a common signaling component for plant immunity mediated by different RLKs. In addition, we showed that cell death in *bir1-1* and PAMP-triggered defense responses are severely attenuated in the *agg1 agg2* double mutant, suggesting that the $G\gamma$ subunits *AGG1* and *AGG2* also play important roles in the regulation of cell death and PAMP-triggered immunity.

According to the classic paradigm, active G proteins dissociate into two functional signaling elements, the $G\alpha$ subunit and the $G\beta\gamma$ dimer. Although it was initially believed that signaling only occurred via the $G\alpha$ subunit, it is now clear that the $G\beta\gamma$ dimer is actively signaling in as many processes as the $G\alpha$ subunit

Five-week-old plants were inoculated by spraying with a bacterial suspension at $OD_{600} = 0.2$. Samples were collected 3 d post inoculation to determine the bacterial titers. Asterisks above the bars indicate significant difference from the wild type ($*P < 0.01$). WT, Wild type. [See online article for color version of this figure.]

(Clapham and Neer, 1997). Plant $G\beta$ and $G\gamma$ interact with each other in vitro and in vivo (Mason and Botella, 2000, 2001; Kato et al., 2004). Our results suggest that the $G\beta\gamma$ dimer acts alone in regulating PAMP-triggered defense responses and cell death in *bir1-1* and that the $G\alpha$ subunit does not play an active role in these processes. This kind of signaling mechanism by G proteins, in which only the $G\beta\gamma$ dimer is involved in the propagation of the signal, was named “classical route II” (Pandey et al., 2010). It can be used to explain the expression patterns of some abscisic acid-regulated genes in guard cells as well as roles of the $G\beta\gamma$ dimers in resistance against necrotrophic pathogens (Pandey et al., 2010; Delgado-Cerezo et al., 2012).

It will be important to determine the roles of the different γ -subunits in PAMP-mediated resistance and whether they confer specificity against different PAMP signals. Although our study has mostly shown redundant roles for AGG1 and AGG2, for some responses, such as elf18-induced oxidative burst, AGG1 seems to play the leading role. A recent report has described the third $G\gamma$ subunit in Arabidopsis, AGG3, with astonishing structural features never before seen in other plant or animal γ -subunits (Chakravorty et al., 2011). AGG3 is involved in stomatal ion channel regulation and development of reproductive organs and has no effect on resistance to *F. oxysporum* (Chakravorty et al., 2011). Our results suggest that AGG3 is probably not involved in PAMP-mediated defense either.

Plant heterotrimeric G proteins have been implicated in the regulation of a wide range of biological processes, yet the receptors that function upstream of G proteins in these processes are still poorly understood. Our study suggests that SOBIR1 and possibly other RLKs, such as FLS2, EFR, and CERK1, function upstream of AGB1 and AGG1/AGG2 to regulate cell death and plant immunity. It is very interesting that AGB1 and AGG1/AGG2 function not only as positive regulators of cell death in *bir1-1*, but also as essential components of PAMP-triggered immunity. One possibility is that there is a common signaling pathway downstream of SOBIR1 and the PAMP receptors FLS2, EFR, and CERK1 that is dependent on AGB1 and AGG1/AGG2. Constitutive activation of this signaling pathway in *bir1-1* results in strong defense responses and activation of cell death, whereas treatment with PAMP signals induces weaker defense responses that do not cause cell death.

Another RLK that may function upstream of AGB1 is ER. *agb1-1* was originally identified in a screen to look for mutants with an *erecta* (*er*) phenotype to find proteins that function together with the RLKs ER in the control of plant development (Lease et al., 2001). *agb1* and *er* mutants share similar fruit phenotypes, and they all have round leaves and shorter stems. Similar to AGB1, ER is also required for resistance against *P. cucumerina* (Llorente et al., 2005). Recently, both *er* and *agb1* mutants were found to have altered cell wall

structure (Sánchez-Rodríguez et al., 2009; Klopffleisch et al., 2011; Delgado-Cerezo et al., 2012). The similarity of the mutant phenotypes in *er* and *agb1* mutants suggests that AGB1 may be required for the functions of ER in the regulation of development, cell wall structure, and resistance against *P. cucumerina*.

agb1 mutant plants exhibit a number of developmental phenotypes, including rounder leaves. One question is whether the altered leaf morphology affects plant immune responses. The rounder leaf morphology is also present in *agg3*, but not in *agg1*, *agg2*, and *agg1 agg2* mutants (Trusov et al., 2006; Chakravorty et al., 2011). Because attenuation of PAMP-triggered defense responses was observed in *agb1* and *agg1 agg2*, but not in *agg3* mutants, the rounder leaf morphology probably does not contribute to the loss of PAMP-triggered immunity in *agb1* mutants.

The $G\alpha$ subunit GPA1 was previously shown to play an important role in stomatal defense against bacterial pathogens. Growth of the coronatine-deficient *P. syringae* pv *tomato* DC3118 is dramatically increased in *gpa1* mutant plants (Zeng and He, 2010). When *agb1* and *agg1 agg2* mutants were inoculated with *P. syringae* pv *tomato* DC3118 by spraying, they supported a small but significant increase of *P. syringae* pv *tomato* DC3118 growth compared with the wild type, suggesting that stomatal defense could be affected in these mutants as well. In *agb1* mutants, stomatal density was shown to be higher than in the wild type (Zhang et al., 2008a; Klopffleisch et al., 2011). The increased stomatal density is probably also a contributing factor to higher *P. syringae* pv *tomato* DC3118 growth in the *agb1* mutants.

AGB1 and AGG1 are colocalized to the plasma membrane (Adjobo-Hermans et al., 2006), suggesting that they may function together with RLKs such as SOBIR1, FLS2, EFR, and CERK1 at the plasma membrane. Preliminary experiments by our research team failed to detect any interaction between the $G\alpha$ / $G\beta$ / $G\gamma$ subunits and the kinase domains of SOBIR1, FLS2, EFR, CERK1, and BAK1 in yeast two-hybrid assays and bifluorescence complementation analysis, suggesting that additional components could be involved in transducing defense signals from the RLKs to $G\beta$ / $G\gamma$ at the plasma membrane.

Recently, the MAPK/ERK KINASE KINASE1 (MEKK1)-MITOGEN ACTIVATED PROTEIN KINASE KINASE1 (MKK1)/MKK2-MPK4 kinase cascade was shown to positively regulate basal resistance against pathogens (Zhang et al., 2012b). We found that activation of MPK4, but not MPK3 and MPK6, was reduced in *agb1* and *agg1 agg2* mutants, suggesting that compromised activation of MPK4 is at least partly responsible for the loss of PAMP-triggered immunity in these mutants. Because blocking activation of MPK4 by mutations in its upstream kinases MEKK1 and MKK1/MKK2 does not affect flg22-induced oxidative burst (Zhang et al., 2012b), AGB1 and AGG1/AGG2 are most likely also involved in activation of defense pathways that are independent of MPK4. Multiple CDPKs

functioning in a MAPK-independent pathway have been shown to be required for flg22-induced resistance against *P. syringae* pv *tomato* DC3000 (Boudsocq et al., 2010). It will be interesting to determine whether AGB1 and AGG1/AGG2 is required for activation of defense responses mediated by these CDPKs.

Our study suggests that heterotrimeric G-protein subunits AGB1 and AGG1/AGG2 function downstream of multiple RLKs, including SOBIR1, FLS2, EFR, and CERK1, to activate resistance responses against pathogens. We hypothesize that RLKs functioning upstream of the plant heterotrimeric G proteins may fulfill the roles of GPCRs in fungi and animals. How the $G\beta\gamma$ dimer is activated by the RLKs remains to be determined. It is also unclear how AGB1 and AGG1/AGG2 regulate downstream defense responses. Identification of downstream target proteins of AGB1 and AGG1/AGG2 should lead to a better understanding of the underlying mechanism of RLK-mediated immunity.

MATERIALS AND METHODS

Plant Material

bir1-1, *bir1-1 pad4-1*, and the 35S-*SOBIR1* transgenic line 2 were previously described (Gao et al., 2009). The *sobir2-1 bir1-1 pad4-1* triple mutant was identified from an ethyl methanesulfonate-mutagenized *bir1-1 pad4-1* population by looking for mutants that can grow to maturity and set seeds at 23°C. *gpa1-3*, *gpa1-4*, and *agb1-2* were provided by Ligeng Ma at the National Institute of Biological Sciences. *agg1-1c*, *agg2-1*, *agg1-1c agg2-1*, *agg3-1*, and *agg3-2* were described previously (Trusov et al., 2007; Chakravorty et al., 2011). *agg1-1c* was obtained by backcrossing *agg1-1w* with wild-type Columbia eight times. The *agg1-1c* and *agg1-1c agg2-1* mutants were backcrossed one more time with Columbia plants to identify mutant plants with homozygous Columbia-*FLS2*. All other mutants used in this study are also in the Columbia background.

For transgene complementation analysis, a 2.9-kb genomic DNA fragment containing *AGB1* lacking the stop codon was amplified by PCR and cloned into a modified pCAMBIA1305 vector with a 3xFLAG tag to obtain pCAMBIA1305-*AGB1*-3xFLAG for expressing the *AGB1*-3xFLAG fusion protein under its native promoter. The plasmid was transformed into *Agrobacterium tumefaciens* and subsequently into the *agb1-2* by floral dipping (Clough and Bent, 1998).

Mutant Characterization

For trypan blue staining, 2-week-old seedlings grown on one-half-strength Murashige and Skoog (MS) plates were placed in microcentrifuge tubes containing 1 mL lactophenol trypan blue solution (10 mg trypan blue, 10 g phenol, 10 mL lactic acid, 10 mL glycerol, and 10 mL water) diluted 1:1 in ethanol and boiled for 2 min. After removing the staining solution, the samples were destained with 1.5 mL chloral hydrate solution (2.5 g mL⁻¹ water) for 2 h and a second time overnight on an orbital shaker. The destained samples were kept in 70% (v/v) glycerol and examined by microscopy.

For 3,3'-diaminobenzidine staining, 2-week-old seedlings grown on one-half-strength MS plates were submerged in 2 mL 3,3'-diaminobenzidine solutions (1 mg mL⁻¹, pH 3.8) in a 24-well tissue culture plate. The samples were vacuumed for 2 min before incubating on an orbital shaker for 1 h. After removing the staining solution, the samples were destained with 95% (v/v) ethanol and examined by microscopy.

For gene expression analysis, RNA was extracted from 2-week-old seedlings grown on one-half-strength MS plates and reverse transcribed to obtain total complementary DNA. Real-time PCR was subsequently performed using the complementary DNA as template to determine the expression levels of the target genes. Primers used for amplification of *PR1*, *PR2*, and *Actin1* were described previously (Zhang et al., 2003).

Infection of *Hyaloperonospora arabidopsidis* Noco2 was carried out by spraying 2-week-old seedlings with spore suspensions at a concentration of 50,000 spores per mL water. The plants were kept at 18°C under 12-h day/12-h night cycles in a growth chamber with 95% humidity. Infection was scored 7 d later as previously described (Bi et al., 2010).

SA was extracted and quantified as previously described (Li et al., 1999). The FLS2 antibodies (Zhang et al., 2010) were provided by Jianmin Zhou. The anti-Erk1/2 antibody specific for the phosphorylated MAPKs was from Cell Signaling Technology (no. 4370). The anti-MPK4 antibody was from Sigma. MPK4 immunocomplex kinase assays were carried out as previously described (Gao et al., 2008).

Elicitor Protection Assays

For elicitor protection assays, 5- to 6-week-old plants grown at 23°C under short-day conditions (10-h day/14-h night cycles) were used. Two leaves from each plant were preinfiltrated with 1 μM flg22, 1 μM elf18, or 200 μg mL⁻¹ chitin. Control plants were infiltrated with distilled, deionized water. The same leaves were subsequently infiltrated with *Pseudomonas syringae* pv *tomato* DC3000 (optical density at 600 nm [OD₆₀₀] = 0.001) in 10 mM MgCl₂ 24 h later. One leaf disc was taken from each infiltrated leaf, and the two leaf discs from the same plant were mixed as one sample. The samples were ground, diluted in 10 mM MgCl₂, and plated on King's B medium. After incubation at 28°C for 2 d, bacterial colonies were counted, and colony-forming units were calculated.

Measurement of Oxidative Burst

Leaf strips with a size of approximately 3 × 5 mm from 5- to 6-week-old plants grown under short-day conditions were placed in a 96-well plate, with each well containing 200 μL water. After incubation at room temperature for about 12 h, the liquid was removed, and 180 μL elicitor solution containing 20 μM luminol, 10 μg mL⁻¹ horseradish peroxidase, and 1 μM flg22, 1 μM elf18, or 200 mg mL⁻¹ chitin was added to each sample. Luminescence was recorded using a GLOMAX 96 microplate luminometer (Promega).

Supplemental Data

The following materials are available in the online version of this article.

Supplemental Figure S1. Map-based cloning of *sobir2-1*.

Supplemental Figure S2. Semiquantitative RT-PCR analysis of *AGB1* expression in the wild type, *agb1-4*, and *agb1-2*.

Supplemental Figure S3. DAB staining of wild-type, *bir1-1*, *agb1-4 bir1-1*, and *agb1-2 bir1-1* mutant seedlings.

Supplemental Figure S4. Semiquantitative RT-PCR analysis of *SOBIR1* expression in the wild type, 35S-*SOBIR1* transgenic line #2 (*SOBIR1 OX-2*), and *agb1-2* carrying the 35S-*SOBIR1* transgene from line #2 (*agb1-2 SOBIR1 OX-2*).

Supplemental Figure S5. FLS2 protein levels in the wild type, *agb1-4*, and *agb1-2*.

Supplemental Figure S6. Activation of MPK3 and MPK6 in mature leaves of the wild type and *agb1-2* by flg22.

Supplemental Figure S7. Induction of *FRK1* and *WRKY29* by flg22 in the wild type, *agb1-2*, and *agb1-2* expressing a wild-type *AGB1* transgene (*agb1/AGB1*).

Supplemental Figure S8. Induction of *GST1* by flg22 is not affected in *agb1-2*.

Supplemental Figure S9. Morphology of wild-type, *bir1-2*, *gpa1-3 bir1-1*, and *gpa1-4 bir1-1* plants.

Supplemental Figure S10. Activation of MPK3 and MPK6 in the wild type, *agg1-1c*, *agg2-1*, and *agg1-1c agg2-1* by flg22.

Supplemental Figure S11. Induction of *GST1* expression in wild-type, *agg1-1c*, *agg2-1*, and *agg1-1c agg2-1* plants.

Supplemental Figure S12. AGG3 is not required for PAMP-triggered immunity.

ACKNOWLEDGMENTS

We thank Ligeng Ma (National Institute of Biological Sciences, Beijing [NIBS]) and the Arabidopsis Biological Resource Center for mutant seeds, Jianmin Zhou (NIBS) for the FLS2 antibodies, Junrong Yang (NIBS) for technical assistance, and Kaeli Johnson (University of British Columbia) for careful reading and discussion of the manuscript.

Received December 7, 2012; accepted February 8, 2013; published February 19, 2013.

LITERATURE CITED

- Adjobo-Hermans MJ, Goedhart J, Gadella TW Jr (2006) Plant G protein heterotrimers require dual lipidation motifs of Galpha and Ggamma and do not dissociate upon activation. *J Cell Sci* **119**: 5087–5097
- Asai T, Tena G, Plotnikova J, Willmann MR, Chiu WL, Gomez-Gomez L, Boller T, Ausubel FM, Sheen J (2002) MAP kinase signalling cascade in Arabidopsis innate immunity. *Nature* **415**: 977–983
- Bi D, Cheng YT, Li X, Zhang Y (2010) Activation of plant immune responses by a gain-of-function mutation in an atypical receptor-like kinase. *Plant Physiol* **153**: 1771–1779
- Boller T, Felix G (2009) A renaissance of elicitors: perception of microbe-associated molecular patterns and danger signals by pattern-recognition receptors. *Annu Rev Plant Biol* **60**: 379–406
- Boudsocq M, Willmann MR, McCormack M, Lee H, Shan L, He P, Bush J, Cheng SH, Sheen J (2010) Differential innate immune signalling via Ca²⁺ sensor protein kinases. *Nature* **464**: 418–422
- Caplan JL, Zhu X, Mamillapalli P, Marathe R, Anandalakshmi R, Dinesh-Kumar SP (2009) Induced ER chaperones regulate a receptor-like kinase to mediate antiviral innate immune response in plants. *Cell Host Microbe* **6**: 457–469
- Chakravorty D, Trusov Y, Zhang W, Acharya BR, Sheahan MB, McCurdy DW, Assmann SM, Botella JR (2011) An atypical heterotrimeric G-protein γ -subunit is involved in guard cell K⁺-channel regulation and morphological development in Arabidopsis thaliana. *Plant J* **67**: 840–851
- Chinchilla D, Zipfel C, Robatzek S, Kemmerling B, Nürnberger T, Jones JD, Felix G, Boller T (2007) A flagellin-induced complex of the receptor FLS2 and BAK1 initiates plant defence. *Nature* **448**: 497–500
- Clapham DE, Neer EJ (1997) G protein beta gamma subunits. *Annu Rev Pharmacol Toxicol* **37**: 167–203
- Clough SJ, Bent AF (1998) Floral dip: a simplified method for Agrobacterium-mediated transformation of Arabidopsis thaliana. *Plant J* **16**: 735–743
- Delgado-Cerezo M, Sánchez-Rodríguez C, Escudero V, Miedes E, Fernández PV, Jordá L, Hernández-Blanco C, Sánchez-Vallet A, Bednarek P, Schulze-Lefert P, et al (2012) Arabidopsis heterotrimeric G-protein regulates cell wall defense and resistance to necrotrophic fungi. *Mol Plant* **5**: 98–114
- Gao M, Liu J, Bi D, Zhang Z, Cheng F, Chen S, Zhang Y (2008) MEKK1, MKK1/MKK2 and MPK4 function together in a mitogen-activated protein kinase cascade to regulate innate immunity in plants. *Cell Res* **18**: 1190–1198
- Gao M, Wang X, Wang D, Xu F, Ding X, Zhang Z, Bi D, Cheng YT, Chen S, Li X, et al (2009) Regulation of cell death and innate immunity by two receptor-like kinases in Arabidopsis. *Cell Host Microbe* **6**: 34–44
- Gimenez-Ibanez S, Hann DR, Ntoukakis V, Petutschnig E, Lipka V, Rathjen JP (2009) AvrPtoB targets the LysM receptor kinase CERK1 to promote bacterial virulence on plants. *Curr Biol* **19**: 423–429
- Gómez-Gómez L, Boller T (2000) FLS2: an LRR receptor-like kinase involved in the perception of the bacterial elicitor flagellin in Arabidopsis. *Mol Cell* **5**: 1003–1011
- Gookin TE, Kim J, Assmann SM (2008) Whole proteome identification of plant candidate G-protein coupled receptors in Arabidopsis, rice, and poplar: computational prediction and in-vivo protein coupling. *Genome Biol* **9**: R120
- Heese A, Hann DR, Gimenez-Ibanez S, Jones AM, He K, Li J, Schroeder JI, Peck SC, Rathjen JP (2007) The receptor-like kinase SERK3/BAK1 is a central regulator of innate immunity in plants. *Proc Natl Acad Sci USA* **104**: 12217–12222
- Ishikawa A (2009) The Arabidopsis G-protein beta-subunit is required for defense response against Agrobacterium tumefaciens. *Biosci Biotechnol Biochem* **73**: 47–52
- Jiang K, Frick-Cheng A, Trusov Y, Delgado-Cerezo M, Rosenthal DM, Lorek J, Panstruga R, Booker FL, Botella JR, Molina A, Ort DR, et al (2012) Dissecting Arabidopsis G β signal transduction on the protein surface. *Plant Physiol* **159**: 975–983
- Kato C, Mizutani T, Tamaki H, Kumagai H, Kamiya T, Hirobe A, Fujisawa Y, Kato H, Iwasaki Y (2004) Characterization of heterotrimeric G protein complexes in rice plasma membrane. *Plant J* **38**: 320–331
- Kloppfleisch K, Phan N, Augustin K, Bayne RS, Booker KS, Botella JR, Carpita NC, Carr T, Chen JG, Cooke TR, et al (2011) Arabidopsis G-protein interactome reveals connections to cell wall carbohydrates and morphogenesis. *Mol Syst Biol* **7**: 532
- Lease KA, Wen J, Li J, Doke JT, Liscum E, Walker JC (2001) A mutant Arabidopsis heterotrimeric G-protein beta subunit affects leaf, flower, and fruit development. *Plant Cell* **13**: 2631–2641
- Lee SW, Han SW, Sriyanyum M, Park CJ, Seo YS, Ronald PC (2009) A type I-secreted, sulfated peptide triggers XA21-mediated innate immunity. *Science* **326**: 850–853
- Li J, Zhao-Hui C, Batoux M, Nekrasov V, Roux M, Chinchilla D, Zipfel C, Jones JD (2009) Specific ER quality control components required for biogenesis of the plant innate immune receptor EFR. *Proc Natl Acad Sci USA* **106**: 15973–15978
- Li X, Zhang Y, Clarke JD, Li Y, Dong X (1999) Identification and cloning of a negative regulator of systemic acquired resistance, SN1, through a screen for suppressors of npr1-1. *Cell* **98**: 329–339
- Liu X, Yue Y, Li B, Nie Y, Li W, Wu WH, Ma L (2007) A G protein-coupled receptor is a plasma membrane receptor for the plant hormone abscisic acid. *Science* **315**: 1712–1716
- Llorente F, Alonso-Blanco C, Sánchez-Rodríguez C, Jorda L, Molina A (2005) ERECTA receptor-like kinase and heterotrimeric G protein from Arabidopsis are required for resistance to the necrotrophic fungus Plectosphaerella cucumerina. *Plant J* **43**: 165–180
- Lu D, Wu S, Gao X, Zhang Y, Shan L, He P (2010) A receptor-like cytoplasmic kinase, BIK1, associates with a flagellin receptor complex to initiate plant innate immunity. *Proc Natl Acad Sci USA* **107**: 496–501
- Lu X, Tintor N, Mentzel T, Kombrink E, Boller T, Robatzek S, Schulze-Lefert P, Saijo Y (2009) Uncoupling of sustained MAMP receptor signaling from early outputs in an Arabidopsis endoplasmic reticulum glucosylase II allele. *Proc Natl Acad Sci USA* **106**: 22522–22527
- Mason MG, Botella JR (2000) Completing the heterotrimer: isolation and characterization of an Arabidopsis thaliana G protein gamma-subunit cDNA. *Proc Natl Acad Sci USA* **97**: 14784–14788
- Mason MG, Botella JR (2001) Isolation of a novel G-protein gamma-subunit from Arabidopsis thaliana and its interaction with Gbeta. *Biochim Biophys Acta* **1520**: 147–153
- Melotto M, Underwood W, Kocza'n J, Nomura K, He SY (2006) Plant stomata function in innate immunity against bacterial invasion. *Cell* **126**: 969–980
- Miya A, Albert P, Shinya T, Desaki Y, Ichimura K, Shirasu K, Narusaka Y, Kawakami N, Kaku H, Shibuya N (2007) CERK1, a LysM receptor kinase, is essential for chitin elicitor signaling in Arabidopsis. *Proc Natl Acad Sci USA* **104**: 19613–19618
- Morillo SA, Tax FE (2006) Functional analysis of receptor-like kinases in monocots and dicots. *Curr Opin Plant Biol* **9**: 460–469
- Nekrasov V, Li J, Batoux M, Roux M, Chu ZH, Lacombe S, Rougon A, Bittel P, Kiss-Papp M, Chinchilla D, et al (2009) Control of the pattern-recognition receptor EFR by an ER protein complex in plant immunity. *EMBO J* **28**: 3428–3438
- Pandey S, Nelson DC, Assmann SM (2009) Two novel GPCR-type G proteins are abscisic acid receptors in Arabidopsis. *Cell* **136**: 136–148
- Pandey S, Wang RS, Wilson L, Li S, Zhao Z, Gookin TE, Assmann SM, Albert R (2010) Boolean modeling of transcriptome data reveals novel modes of heterotrimeric G-protein action. *Mol Syst Biol* **6**: 372
- Perfus-Barbeoch L, Jones AM, Assmann SM (2004) Plant heterotrimeric G protein function: insights from Arabidopsis and rice mutants. *Curr Opin Plant Biol* **7**: 719–731
- Saijo Y, Tintor N, Lu X, Rauf P, Pajerowska-Mukhtar K, Häweker H, Dong X, Robatzek S, Schulze-Lefert P (2009) Receptor quality control in the endoplasmic reticulum for plant innate immunity. *EMBO J* **28**: 3439–3449
- Sánchez-Rodríguez C, Estévez JM, Llorente F, Hernández-Blanco C, Jordá L, Pagán I, Berrocal M, Marco Y, Somerville S, Molina A (2009) The ERECTA receptor-like kinase regulates cell wall-mediated resistance

- to pathogens in *Arabidopsis thaliana*. *Mol Plant Microbe Interact* **22**: 953–963
- Shiu SH, Bleecker AB** (2001) Receptor-like kinases from *Arabidopsis* form a monophyletic gene family related to animal receptor kinases. *Proc Natl Acad Sci USA* **98**: 10763–10768
- Song WY, Wang GL, Chen LL, Kim HS, Pi LY, Holsten T, Gardner J, Wang B, Zhai WX, Zhu LH, et al** (1995) A receptor kinase-like protein encoded by the rice disease resistance gene, Xa21. *Science* **270**: 1804–1806
- Suharsono U, Fujisawa Y, Kawasaki T, Iwasaki Y, Satoh H, Shimamoto K** (2002) The heterotrimeric G protein alpha subunit acts upstream of the small GTPase Rac in disease resistance of rice. *Proc Natl Acad Sci USA* **99**: 13307–13312
- Temple BR, Jones AM** (2007) The plant heterotrimeric G-protein complex. *Annu Rev Plant Biol* **58**: 249–266
- Trujillo M, Ichimura K, Casais C, Shirasu K** (2008) Negative regulation of PAMP-triggered immunity by an E3 ubiquitin ligase triplet in *Arabidopsis*. *Curr Biol* **18**: 1396–1401
- Trusov Y, Rookes JE, Chakravorty D, Armour D, Schenk PM, Botella JR** (2006) Heterotrimeric G proteins facilitate *Arabidopsis* resistance to necrotrophic pathogens and are involved in jasmonate signaling. *Plant Physiol* **140**: 210–220
- Trusov Y, Rookes JE, Tilbrook K, Chakravorty D, Mason MG, Anderson D, Chen JG, Jones AM, Botella JR** (2007) Heterotrimeric G protein γ subunits provide functional selectivity in $G\beta\gamma$ dimer signaling in *Arabidopsis*. *Plant Cell* **19**: 1235–1250
- Trusov Y, Sewelam N, Rookes JE, Kunkel M, Nowak E, Schenk PM, Botella JR** (2009) Heterotrimeric G proteins-mediated resistance to necrotrophic pathogens includes mechanisms independent of salicylic acid-, jasmonic acid/ethylene- and abscisic acid-mediated defense signaling. *Plant J* **58**: 69–81
- Wan J, Zhang XC, Neece D, Ramonell KM, Clough S, Kim SY, Stacey MG, Stacey G** (2008) A LysM receptor-like kinase plays a critical role in chitin signaling and fungal resistance in *Arabidopsis*. *Plant Cell* **20**: 471–481
- Zeng W, He SY** (2010) A prominent role of the flagellin receptor FLAGELLIN-SENSING2 in mediating stomatal response to *Pseudomonas syringae* pv *tomato* DC3000 in *Arabidopsis*. *Plant Physiol* **153**: 1188–1198
- Zhang H, Wang M, Wang W, Li D, Huang Q, Wang Y, Zheng X, Zhang Z** (2012a) Silencing of G proteins uncovers diversified plant responses when challenged by three elicitors in *Nicotiana benthamiana*. *Plant Cell Environ* **35**: 72–85
- Zhang J, Li W, Xiang T, Liu Z, Laluk K, Ding X, Zou Y, Gao M, Zhang X, Chen S, et al** (2010) Receptor-like cytoplasmic kinases integrate signaling from multiple plant immune receptors and are targeted by a *Pseudomonas syringae* effector. *Cell Host Microbe* **7**: 290–301
- Zhang L, Hu G, Cheng Y, Huang J** (2008a) Heterotrimeric G protein alpha and beta subunits antagonistically modulate stomatal density in *Arabidopsis thaliana*. *Dev Biol* **324**: 68–75
- Zhang W, He SY, Assmann SM** (2008b) The plant innate immunity response in stomatal guard cells invokes G-protein-dependent ion channel regulation. *Plant J* **56**: 984–996
- Zhang Y, Tessaro MJ, Lassner M, Li X** (2003) Knockout analysis of *Arabidopsis* transcription factors *TGA2*, *TGA5*, and *TGA6* reveals their redundant and essential roles in systemic acquired resistance. *Plant Cell* **15**: 2647–2653
- Zhang Z, Wu Y, Gao M, Zhang J, Kong Q, Liu Y, Ba H, Zhou J, Zhang Y** (2012b) Disruption of PAMP-induced MAP kinase cascade by a *Pseudomonas syringae* effector activates plant immunity mediated by the NB-LRR protein SUMM2. *Cell Host Microbe* **11**: 253–263
- Zipfel C, Kunze G, Chinchilla D, Caniard A, Jones JD, Boller T, Felix G** (2006) Perception of the bacterial PAMP EF-Tu by the receptor EFR restricts *Agrobacterium*-mediated transformation. *Cell* **125**: 749–760